First-order chiral phase transition in high-energy collisions: Can nucleation prevent spinodal decomposition?

O. Scavenius,[1,2] A. Dumitru,[3] E. S. Fraga,[4] J. T. Lenaghan,[2,5] and A. D. Jackson[2]

[1]*NORDITA, Blegdamsvel 17, DK-2100 Copenhagen Ø, Denmark*
[2]*The Niels Bohr Institute, Blegdamsvej 17, DK-2100 Copenhagen Ø, Denmark*
[3]*Department of Physics, Columbia University, New York, New York 10027*
[4]*Department of Physics, Brookhaven National Laboratory, Upton, New York 11973-5000*
[5]*Department of Physics, Yale University, New Haven, Connecticut 06520*

We discuss homogeneous nucleation in a first-order chiral phase transition within an effective field theory approach to low-energy QCD. Exact decay rates and bubble profiles are obtained numerically and compared to analytic results obtained with the thin-wall approximation. The thin-wall approximation overestimates the nucleation rate for any degree of supercooling. The time scale for critical thermal fluctuations is calculated and compared to typical expansion times for high-energy hadronic or heavy-ion collisions. We find that significant supercooling is possible, and the relevant mechanism for phase conversion might be that of spinodal decomposition. Some potential experimental signatures of supercooling, such as an increase in the correlation length of the scalar condensate, are also discussed.

I. INTRODUCTION

It is hoped that experiments in the near future at BNL Relativistic Heavy Ion Collider (RHIC) and CERN Large Hadron Collider (LHC) will discover evidence for the so-called quark-gluon plasma (QGP) in high-energy collisions of heavy-ions or protons [1]. The QGP is the high-density primordial state of strongly interacting matter that presumably existed in the early universe a few microseconds after the big bang [2,3]. In the QGP, chiral symmetry is restored due to finite-temperature contributions to the effective potential [4]. (This statement is only approximate since finite current-quark masses break chiral symmetry explicitly. See below.)

Given our lack of detailed quantitative knowledge regarding low energy QCD, it is difficult to identify unambiguous observables that would, if found, demonstrate beyond reasonable doubt that the QGP had been produced. Central ultrarelativistic collisions of heavy ions at RHIC and LHC will produce multiplicities on the order of 10^4 hadrons per event [5] and raise the possibility of analyzing data event-by-event [6]. Event-by-event fluctuations might provide an opportunity to discover new physics that is usually washed out by standard event averaging. In particular, if the phase transition is first-order with fast expansion so that strong supercooling or spinodal decomposition is possible, fluctuations in the rapidity density or in the transverse momentum spectra of hadrons and isospin fluctuations produced by the formation of domains of a coherent chiral condensate [7–9] could become interesting observables.

The nature of the QCD phase diagram in the temperature T and baryon chemical potential μ plane has been intensively studied in recent years [10,11]. Random matrix and effective model calculations suggest that, at low μ and non-zero T, a smooth crossover transition is expected and that, at low T and non-zero μ, the chiral phase transition should be of first order. Thus, a second-order critical point must exist inbetween these two limits. The arguments suggesting this topology for the phase diagram are in no sense complete, and the phase transition could also be first-order for $\mu=0$.

In a first-order phase transition, the thermodynamic potential exhibits a metastable minimum corresponding to the symmetry restored phase for temperatures slightly less than the critical temperature T_c. This minimum gradually disappears as the system cools and ends at a point of inflection, i.e., a ''spinodal instability.'' In a slowly expanding system, the phase transition would proceed through the nucleation of bubbles of the ''true vacuum'' state via thermal activation [3,12–16,18]. In ultrarelativistic collisions of heavy ions or hadrons, it is clear that expansion is very fast compared to that of the early universe at the cosmological QCD transition (by a factor of $\sim 10^{18}$: $H \simeq 10^{23}$ sec^{-1} versus $H \simeq 10^5$ sec^{-1}). Thus, it is necessary to investigate the time scale for thermal nucleation relative to that for expansion to see if the metastable chirally symmetric state of matter can reach the spinodal instability before nucleation is completed.

In this paper we shall consider a first-order chiral phase transition in a rapidly expanding background. We take a linear σ-model coupled to quarks as our effective theory. Treating the quarks as a heat bath which generates an effective potential for the soft modes of the chiral order parameter, we obtain an effective potential at the one-loop level. Somewhat below the critical temperature, this slightly asymmetric effective potential has three local minima. Starting with the order parameter ''localized'' in the metastable chirally symmetric state of matter, we then study critical bubble profiles and calculate the nucleation rate to the broken symmetry phase. This will provide the temporal and spatial scales of thermal field fluctuations into the broken symmetry state. We will consider both analytical and numerical computations. Our numerical results represent ''exact'' calculations. In the analytical treatment, we must turn to the thin-wall approxi-

mation in order to obtain closed results. The comparison between these two approaches will allow us to establish limits on the reliability of the thin-wall approximation.

This paper is organized as follows. Section II presents our effective theory. Section III describes homogeneous nucleation and the methods used for both numerical and analytic computations of bubble profiles and nucleation rates. Our results are discussed in Sec. IV. Section V presents our conclusions and suggested directions for future investigation. We employ natural units, $\hbar = c = k_B = 1$, throughout.

II. EFFECTIVE THEORY

As an effective theory of the chiral symmetry breaking dynamics, we assume the linear σ-model coupled to quarks [9,19,20]:

$$\mathcal{L} = \bar{q}[i\gamma^\mu \partial_\mu - g(\sigma + i\gamma_5 \vec{\tau} \cdot \vec{\pi})]q$$
$$+ \frac{1}{2}(\partial_\mu \sigma \partial^\mu \sigma + \partial_\mu \vec{\pi} \partial^\mu \vec{\pi}) - U(\sigma, \vec{\pi}). \quad (2.1)$$

The potential, which exhibits both spontaneously and explicitly broken chiral symmetry, is

$$U(\sigma, \vec{\pi}) = \frac{\lambda^2}{4}(\sigma^2 + \vec{\pi}^2 - v^2)^2 - h_q \sigma. \quad (2.2)$$

Here q is the constituent-quark field $q = (u, d)$. The scalar field σ and the pseudoscalar field $\vec{\pi} = (\pi_1, \pi_2, \pi_3)$ together form a chiral field $\Phi = (\sigma, \vec{\pi})$. The parameters of the Lagrangian are chosen such that chiral $SU_L(2) \otimes SU_R(2)$ symmetry is spontaneously broken in the vacuum. The vacuum expectation values of the condensates are $\langle \sigma \rangle = f_\pi$ and $\langle \vec{\pi} \rangle = 0$, where $f_\pi = 93$ MeV is the pion decay constant. The explicit symmetry breaking term is due to the finite current-quark masses and is determined by the PCAC (partial conservation of axial vector coupling) relation which gives $h_q = f_\pi m_\pi^2$, where $m_\pi = 138$ MeV is the pion mass. This leads to $v^2 = f_\pi^2 - m_\pi^2/\lambda^2$. The value of $\lambda^2 = 20$ leads to a σ-mass, $m_\sigma^2 = 2\lambda^2 f_\pi^2 + m_\pi^2$, equal to 600 MeV. In mean field theory, the purely bosonic part of this Lagrangian exhibits a second-order phase transition [21] at $T_c = \sqrt{2}v$ if the explicit symmetry breaking term, h_q, is dropped. For $h_q \neq 0$, the transition becomes a smooth crossover from the restored to broken symmetry phases. For $g > 0$, the finite-temperature one-loop effective potential also includes the following contribution from the quarks:

$$V_q(\Phi) = -d_q T \int \frac{d^3 k}{(2\pi)^3} \log(1 + e^{-E/T}). \quad (2.3)$$

Here, $d_q = 24$ denotes the color-spin-isospin-baryon charge degeneracy of the quarks. We note that $V_q(\Phi)$ depends on the order parameter Φ through the effective mass of the quarks, $m_q = g\sqrt{\Phi^2}$, which enters into the expression for the energy, $E = \sqrt{k^2 + g^2\Phi^2}$. In our phenomenological approach, we will assume that the quarks constitute the heat bath in

which the long-wavelength modes of the chiral field, i.e., the order parameter, evolve. Thus, we will take the effective potential to be

$$V_{\text{eff}} \equiv U + V_q. \quad (2.4)$$

To arrive at this form for the effective potential we consider a system of quarks and antiquarks in thermodynamical equilibrium at temperature T (in [11] V_{eff} is derived also at finite baryon-chemical potential; here we shall consider only the case of baryon-symmetric matter). The partition function reads

$$\mathcal{Z} = \int \mathcal{D}\bar{q}\mathcal{D}q\mathcal{D}\sigma\mathcal{D}\vec{\pi} \exp\left[\int_0^{1/T} d(it) \int_{\mathcal{V}} d^3x \mathcal{L}\right]. \quad (2.5)$$

$\mathcal{V}$ is the volume of the system. In mean-field approximation the chiral fields in the Lagrangian are replaced by their expectation values, which we will denote by σ and $\vec{\pi}$ in the following. Then, up to an overall normalization factor,

$$\mathcal{Z} = \mathcal{N}_U \int \mathcal{D}\bar{q}\mathcal{D}q$$
$$\times \exp\left\{\int_0^{1/T} d(it) \int_{\mathcal{V}} d^3x \bar{q}[i\gamma^\mu \partial_\mu - g(\sigma + i\gamma_5 \vec{\tau} \cdot \vec{\pi})]q\right\}$$
$$= \mathcal{N}_U \det_p\{[p_\mu \gamma^\mu - g(\sigma + i\gamma_5 \vec{\tau} \cdot \vec{\pi})]/T\}, \quad (2.6)$$

where

$$\mathcal{N}_U = \exp\left(-\frac{\mathcal{V}U(\sigma, \vec{\pi})}{T}\right). \quad (2.7)$$

Taking the logarithm of $\mathcal{Z}$, the determinant of the Dirac operator can be evaluated in the standard fashion [22], and we finally obtain the grand canonical potential

$$\Omega(T) = -\frac{T}{\mathcal{V}}\log\mathcal{Z} = U + \tilde{V}_q(T), \quad (2.8)$$

where

$$\tilde{V}_q(T) = -d_q \int \frac{d^3\vec{p}}{(2\pi)^3}\{E + T\log[1 + e^{-E/T}]\}. \quad (2.9)$$

For our purposes, the zero-temperature contribution to $\tilde{V}_q$ can be partly absorbed into U via a standard renormalization of the bare parameters λ^2 and v^2. However, a logarithmic correction from the renormalization scale remains and is neglected in the following (see [11] for more details). The finite-T part defines V_q as given in Eq. (2.3).

We now turn to a discussion of the shape of the effective potential at various temperatures. For sufficiently small g one still finds the above-mentioned smooth transition between the two phases. At larger coupling to the quarks, however, the effective potential exhibits a first-order phase transition. For temperatures near the critical temperature, V_{eff} displays a local minimum $\Phi = \Phi_f(T) \simeq 0$ which is separated by a bar-
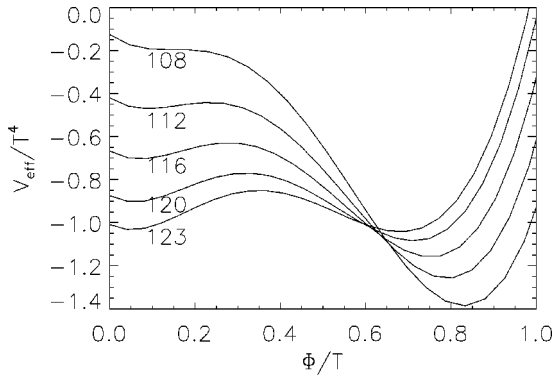
FIG. 1. The one-loop finite-T effective potential for $T_{sp} \lesssim T \lesssim T_c$ and coupling constants $g=5.5$, $\lambda^2=20$. The curves are labeled by the temperature in MeV.

FIG. 2. The one-loop finite-T effective potential for $T_{sp} \lesssim T \lesssim T_c$ and coupling constants $g=10$, $\lambda^2=20$. The curves are labeled by the temperature in MeV.

rier from another local minimum at $\Phi=\Phi_t(T)>0$. (There is another local minimum for negative Φ which is of higher energy and need not concern us.) These two minima are degenerate at $T=T_c$. For example, $g=5.5$ leads to a critical temperature of $T_c=123.7$ MeV. Unless stated differently, throughout the manuscript we shall adopt the values $g=5.5$ for the quark-field coupling and $\lambda^2=20$ for the self-coupling of the chiral fields.

Chiral symmetry is (approximately) restored for $T>T_c$. The minimum at $\Phi=\Phi_t$ becomes the absolute minimum as the temperature is reduced below T_c. As the temperature is lowered, the local minimum at $\Phi \approx 0$ approaches the intervening maximum. These two extrema meet and form an inflection point at the spinodal temperature, T_{sp}. Only the broken symmetry minimum remains for $T<T_{sp}$. For our standard choice of parameters, $T_{sp}=108$ MeV. The potential in the σ-direction is shown in Fig. 1 for the range of interest, $T_{sp} \lesssim T \lesssim T_c$; see also Ref. [9].[1] Note the rather small barrier between the two local minima of V_{eff} at T_c. The first-order transition for $g=5.5$ is weak compared to those conventional in bag model calculations [16]. This weakness is due to the fact that gluons, absent in the present linear σ-model, are treated as free fields (for $T \gtrsim T_c$) in the bag model. It is not our goal here to argue which approximation is more reasonable. Rather, we view our approach as complementary to previous studies which employed the bag model [3,12,16]. The existence of a local minimum in V_{eff} raises the possibility of super-cooling effects since the true broken symmetry minimum can only be reached by tunneling. The weakness of our first-order transition is likely to overestimate tunneling rates and underestimate the effects of supercooling.

In fact, increasing the coupling to the quarks leads to a larger barrier between the two local minima of the effective potential, as seen in Fig. 2. In other words, the first-order transition becomes stronger, with larger latent heat. Furthermore, the spinodal temperature T_{sp} decreases considerably, to about $\simeq 78$ MeV. As will become clear below, both ef-
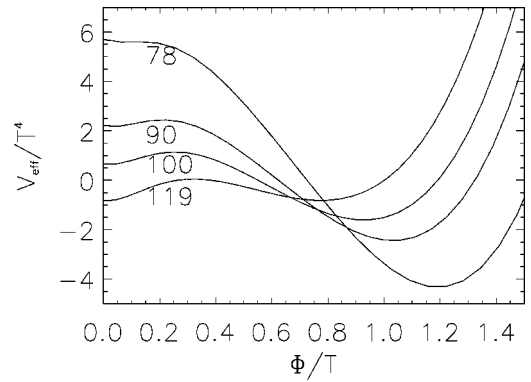
fects (the higher barrier and the lower temperatures) act to reduce the decay rate of the metastable minimum as compared to our ''standard'' choice of couplings corresponding to the potential shown in Fig. 1.

There is also the possibility that the σ-meson is much lighter at T_c than at $T=0$ [23] (i.e. λ^2 is small) if QCD is near a chiral critical point. Choosing for example $\lambda^2 \simeq 2.2$ with the pion decay constant f_π and vacuum mass m_π fixed, such that $v^2=0$, leads to the potential shown in Fig. 3. Clearly, decreasing λ^2 in this theory reduces T_c very much, to less than 100 MeV. Reducing g has practically no effect, except that the first-order phase transition disappears at $g \lesssim 4$. Such low T_c appear to be excluded by present lattice QCD results [17], and will therefore not be considered further.

In order to obtain approximate analytic formulas, it is convenient to express V_{eff} over the range $0 \leq \Phi \leq T$ in the familiar Landau-Ginzburg form (see also [12])

$$V_{eff} \approx \sum_{n=0}^{4} a_n \Phi^n. \qquad (2.10)$$

This form is adopted purely for reasons of convenience and no deeper meaning should be attached to it. It is, for example, obviously incapable of reproducing all three minima
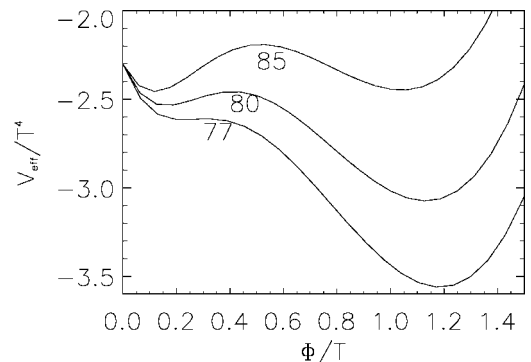

FIG. 3. The one-loop finite-T effective potential for $T_{sp} \lesssim T \lesssim T_c$ and coupling constants $g=5.5$, $\lambda^2=2.2$. The curves are labeled by the temperature in MeV.

---

[1]The right diagram in Fig. 1 of Ref. [9] is incorrectly indicated as corresponding to $T=100$ MeV. It actually represents $T=108$ MeV.

of V_{eff}. We shall use this expansion both for a limited range of temperatures ($T_{\text{sp}} \leq T \leq T_c$) and for a limited range of field strengths ($0 \leq \Phi \leq T$) which includes the two local minima of interest. With these restrictions, this polynomial form is found to provide a quantitative description of V_{eff}. The coefficients a_n are determined for each T by performing a least squares fit to the true effective potential.

III. HOMOGENEOUS NUCLEATION

We wish to consider the physical situation (realizable for $T_{\text{sp}} \leq T \leq T_c$) in which a scalar field, corresponding to the σ-direction, is initially localized in the metastable restored symmetry minimum of an asymmetric double-well potential. (We neglect the higher-energy local minimum with $\Phi < 0$.) It is well known that such a system can decay by the nucleation of thermally activated bubbles of the true vacuum inside the false one [3,12–16,18]. The nucleation rate per unit volume per unit time is expressed as

$$\Gamma = \mathcal{P} e^{-F_b/T}, \tag{3.1}$$

where F_b is the free energy of a critical bubble and where the prefactor $\mathcal{P}$ provides a measure of the saddle point of the Euclidean action in functional space. It is conventional to write $\mathcal{P}$ as a product of the bubble's growth rate and a factor proportional to the ratio of the determinant of the fluctuation operator around the bubble configuration to that around the homogeneous metastable state. The following analysis will concentrate on the exponential barrier penetration factor, and we will approximate $\mathcal{P}$ by T^4. This approximation is known to give an overestimate of Γ, see e.g. [15,16]. The reason for this focus is that F_b is necessarily infinite at T_c and zero at T_{sp}. The exponential factor is thus expected to make the dominant contribution to the structure of Γ.

In order to determine the role of bubble nucleation in the evolving system and to be able to compute the decay rate Γ, it is necessary to study the critical bubble and some of its features. The critical bubble is a radially symmetric, static solution of the Euler-Lagrange field equations that satisfies the boundary condition $\Phi(r \to \infty) \to \Phi_f$ where Φ_f is the false vacuum of the effective potential. Energetically, this boundary condition corresponds to an exact balance between volume and surface contributions which defines the critical radius, $R = R_c$. The critical bubble is unstable with respect to small changes of its radius. For $R < R_c$, the surface energy dominates, and the bubble shrinks into the false vacuum. For $R > R_c$, the volume energy dominates, and the bubble grows driving the decay process.

The critical bubble can be found by minimizing the free energy

$$F_b(\Phi,T) = 4\pi \int r^2 dr \left[\frac{1}{2}\left(\frac{d\Phi}{dr}\right)^2 + V_{\text{eff}}(\Phi,T) \right], \tag{3.2}$$

with respect to the field Φ. This leads to

$$\frac{d^2\Phi}{dr^2} + \frac{2}{r}\frac{d\Phi}{dr} - \frac{\delta V_{\text{eff}}(\Phi,T)}{\delta\Phi} = 0, \tag{3.3}$$

where

$$\frac{\delta V_{\text{eff}}(\Phi,T)}{\delta\Phi} = \lambda(\Phi^2 - v^2)\Phi - h_q$$

$$+ \frac{g^2\Phi d_q}{\pi^2}\int dp \frac{p^2}{E}\frac{1}{\exp(E/T)+1}. \tag{3.4}$$

[It has been assumed in Eq. (3.2) that the effective potential is shifted so that $V_{\text{eff}}(\Phi_f,T) = 0$.] The desired solution of Eq. (3.3) is found by imposing the boundary condition $\Phi(r \to \infty) \to \Phi_f$.

For numerical purposes it is more convenient to impose boundary conditions at $r = 0$ by setting $\Phi'(0) = 0$ and $\Phi(0)$ equal to an "escape value" Φ_e. It is straightforward to integrate Eq. (3.3) to obtain the bubble profile $\Phi(r)$ for a given temperature. The escape value is then adjusted until the desired boundary conditions at $r \to \infty$ are realized. This process can be facilitated by smoothly joining the numerical values of $\Phi(r)$ to the analytic solution to Eq. (3.3) that is regular as $r \to \infty$. Close to the critical temperature, $\Phi(r)$ has a simple qualitative behavior. It stays close the escape value Φ_e for $r < R_c$ and then makes a rapid transition to the false vacuum, Φ_f. For obvious reasons, R_c is identified as the radius of the critical bubble. Once the profile of the critical bubble has been found, the free energy F_b is obtained by computing the integral in Eq. (3.2) numerically. Finally, the decay rate can be calculated using the approximate prefactor $\mathcal{P} = T^4$.

A simple physical analogue of this procedure can be obtained by turning the potentials in Fig. 1 upside down and considering the mechanical motion of a point particle moving in the inverted potential. The problem of determining the critical bubble profile is then seen to be equivalent to finding that point on the true vacuum hill such that a ball starting at rest and obeying the equation of motion, Eq. (3.3), would descend and land at rest on the top of the false vacuum hill at the point Φ_f. The starting point is evidently the escape point. It does not correspond to the true vacuum point but rather to some smaller value. This mechanical analogy also makes it clear that $-V_{\text{eff}}(\Phi_e)$ must be greater than $-V_{\text{eff}}(\Phi_f)$ due to the presence of the second, "frictional" term in Eq. (3.3). As we shall see, the critical radius R_c diverges as $T \to T_c$. The frictional term then becomes small in some sense. The various approximate methods for dealing with this frictional term approximately are all described as "the thin-wall approximation."

Although the thin-wall approximation is not expected to be valid near the spinodal, it should provide a reliable description of nucleation near T_c. Given the frequency of its adoption and its simplicity, we find it useful to apply the thin-wall approximation to the present problem. A quartic potential such as Eq. (2.10) can always be rewritten in the form

$$W(\varphi) = \alpha(\varphi^2 - a^2)^2 + j\varphi. \tag{3.5}$$

Specifically, we have

$$\alpha = a_4, \tag{3.6}$$

$$a^2 = \frac{1}{2}\left[-\frac{a_2}{a_4} + \frac{3}{8}\left(\frac{a_3}{a_4}\right)^2\right], \tag{3.7}$$

$$j = a_4\left[\frac{a_1}{a_4} - \frac{1}{2}\frac{a_2}{a_4}\frac{a_3}{a_4} + \frac{1}{8}\left(\frac{a_3}{a_4}\right)^3\right], \tag{3.8}$$

$$\varphi = \Phi + \frac{1}{4}\frac{a_3}{a_4}. \tag{3.9}$$

The new potential $W(\varphi)$ reproduces the original $V_{eff}(\Phi)$ up to a shift in the zero of energy. We are interested in the effective potential only between T_c and T_{sp}. At T_c, we will have two distinct minima of equal depth. This clearly corresponds to the choice $j=0$ in Eq. (3.5) so that W has minima at $\varphi=\pm a$ and a maximum at $\varphi=0$. The minimum at $\varphi = -a$ and the maximum move closer together as the temperature is lowered and merge at T_{sp}. Thus, the spinodal requires $j/\alpha a^3 = -8/3\sqrt{3}$ in Eq. (3.5). In the present case, the parameter α is essentially independent of temperature, and a rises roughly linearly by some 3% as the temperature falls from T_c to T_{sp}. The parameter $j/\alpha a^3$ falls roughly linearly from 0 (at T_c) to $-8/3\sqrt{3}$ (at T_{sp}).

The explicit form of the critical bubble in the thin-wall limit is then given by [18]

$$\varphi_c(r;\xi,R_c) = \varphi_f + \frac{1}{\xi\sqrt{2\alpha}}\left[1 - \tanh\left(\frac{r-R_c}{\xi}\right)\right], \tag{3.10}$$

where φ_f is the new false vacuum, R_c is the radius of the critical bubble, and $\xi = 2/m$ with $m^2 \equiv W''(\varphi_f)$ is a measure of the wall thickness. The thin-wall limit corresponds to $\xi/R_c \ll 1$ [18], which can be rewritten as $(3|j|/8\alpha a^3) \ll 1$. This small parameter has the value of $1/\sqrt{3}$ at the spinodal, which suggests that the thin-wall approximation might be qualitatively reliable for our purposes. Nevertheless, it merits a quantitative check. In terms of the parameters α, a, and j defined above, we find

$$\varphi_{t,f} \approx \pm a - \frac{j}{8\alpha a^2} \tag{3.11}$$

$$\xi = \left[\frac{1}{\alpha(3\varphi_f^2 - a^2)}\right]^{1/2} \tag{3.12}$$

in the thin-wall limit. Determination of the critical radius requires the surface tension, Σ, defined as

$$\Sigma \equiv \int_0^\infty dr\left(\frac{d\varphi_b}{dr}\right)^2 \approx \frac{2}{3\alpha\xi^3}. \tag{3.13}$$

The critical radius then becomes

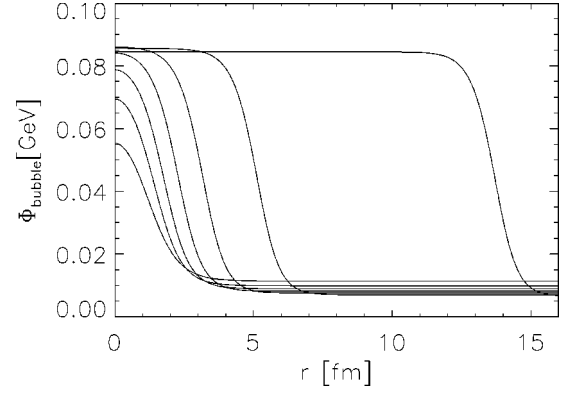$$R_c = \frac{2\Sigma}{\Delta W}, \tag{3.14}$$

where

FIG. 4. Exact bubble profiles for temperatures 110, 112, 114, 116, 118, 120, and 122 MeV. Bubble size increases monotonically with temperature. Recall that $T_c = 123.7$ MeV and $T_{sp} = 108$ MeV.

$$\Delta W \equiv V(\Phi_f) - V(\Phi_t) \approx 2a|j|. \tag{3.15}$$

The energy of a critical bubble is finally given by

$$E_c = \frac{4\pi\Sigma}{3}R_c^2. \tag{3.16}$$

From knowledge of $F_b = E_c$, one can evaluate the nucleation rate Γ. In calculating thin-wall properties, we shall use the approximate forms for ϕ_t, ϕ_f, Σ, and ΔW for all values of the potential parameters.

IV. RESULTS

We begin by showing the critical bubble profiles obtained from the exact numerical solution of Eq. (3.3) in Fig. 4. For small supercooling the bubble profiles exhibit a pronounced "core" with $\Phi \simeq \Phi_t$ separated by a relatively thin wall from the region $\Phi = \Phi_f$. On the other hand, critical bubbles become "coreless" for stronger supercooling; their thickness is of the same order as the radius, and the field at the escape point, $\Phi(r=0)$, does not reach Φ_t. For comparison, Fig. 5 shows bubble profiles for temperatures $T = 110$ and 120 MeV as obtained from the numerical solution of Eq. (3.3) and
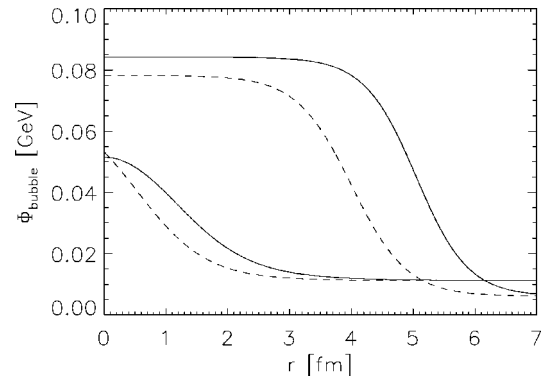

FIG. 5. Critical bubble profiles for temperatures 110 and 120 MeV. The solid line indicates exact numerical results. The dashed line shows the results obtained with the thin-wall approximation.
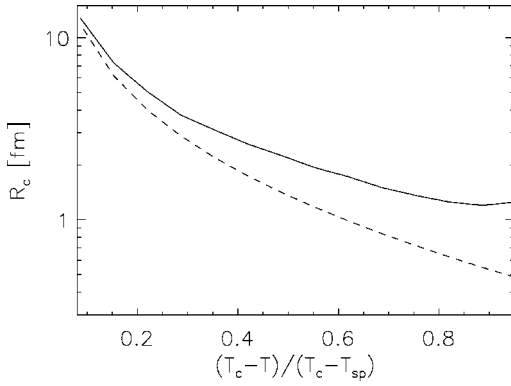
FIG. 6. Critical radii computed numerically (solid line) and with the thin-wall approximation (dashed line) as functions of the degree of supercooling.
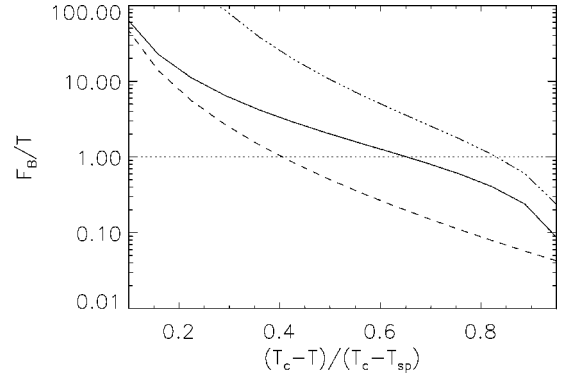

FIG. 7. The free energy of the critical bubbles as a function of the degree of supercooling. The solid line shows the exact (numerical) result, the dashed line shows the thin-wall approximation, and the dotted line shows exact results for the modified effective potential discussed in the text.

from the thin-wall approximation. In this case, we have used the same polynomial approximation to V_{eff} in both exact and thin-wall calculations so that discrepancies can be associated cleanly with the thin-wall approximation. (The critical bubble profile is quite sensitive to the precise form of V_{eff}. This is particularly true when $T \approx T_c$ and the bubble radius is large.) As expected, the thin-wall approximation provides a qualitatively reasonable description of the critical bubble profile.

In Fig. 6, we compare the critical radii R_c obtained from the two calculations as a function of temperature. For the exact numerical calculation, R_c has been extracted from the bubble profile shown in Fig. 4 as the point at which the curvature of the profile changes sign.[2] This figure makes it clear that the thin-wall approximation becomes quantitatively correct as $T \to T_c$ and $R_c \to \infty$ as expected. The fact that the thin-wall approximation systematically underestimates R_c will be reflected in a systematic overestimate of the decay rate of the metastable state.

This expectation is also supported by Fig. 7 which shows F_b/T as a function of the degree of supercooling, x, defined as $x = (T_c - T)/(T_c - T_{\text{sp}})$. This figure also allows us to calibrate the temperature range of primary interest in the present work. We have chosen to concentrate on the relatively violent behavior of the exponential factor in Eq. (3.1) and to treat the prefactor, $\mathcal{P}$, crudely. Given, the dramatic changes in F_b/T as a function of supercooling shown in this figure, this focus seems appropriate. For temperatures such that $F_b/T > 1$, Γ will be strongly suppressed by the exponential factor, and the system is likely to remain in the metastable state for times comparable to the expansion time of the system. For lower temperatures, the exponential factor is unimportant, and Γ is determined primarily by the prefactor, $\mathcal{P}$. At such temperatures, it becomes necessary to make a more detailed comparison of the decay rate with the expansion rate of the system in order to decide the fate of the metastable

state. Such comparison requires a more reliable description of $\mathcal{P}$ than that adopted here. The exact results shown in the figure suggest that the system is likely to supercool for some two-thirds of the way from T_c to T_{sp}. By contrast, the thin-wall results yield the significantly smaller value of $x \approx 0.4$.

Given the weakness of the first-order phase transition predicted by our model with $g = 5.5$, it is remarkable that the system can come so close to the spinodal temperature before the stability of the metastable state is seriously challenged. It is to be expected that effective potentials which maintain the same T_c and T_{sp} but which have a higher barrier between the phases at T_c would permit the metastable state to come even closer to the spinodal temperature.

This point can be illustrated by considering an artificially modified effective potential with a higher barrier. We construct this potential from our quartic approximations by arbitrarily multiplying the parameter j at each temperature by a factor of $(T_c - T)/(T_c - T_{\text{sp}})$. Evidently, this modification has no effect on V_{eff} at the critical temperature (where j is 0) or at the spinodal (where the additional factor is 1). The maximum difference in effective potentials lies halfway between these extremes and is illustrated in Fig. 8. While the difference between these potentials is not dramatically large,
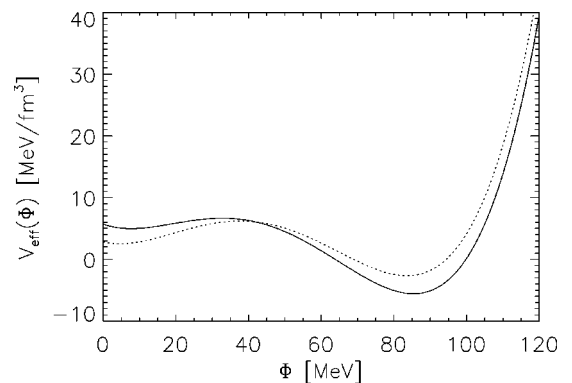

FIG. 8. The effective potential at $T = 116$ MeV. The solid line shows the original V_{eff} from Fig. 1. The dotted line shows the modified V_{eff} as discussed in the text.

---

[2]This definition of R_c is somewhat arbitrary. This figure is intended only for the comparison of exact and thin-wall results. Our numerical calculations do not employ R_c in any of the quantities discussed below.
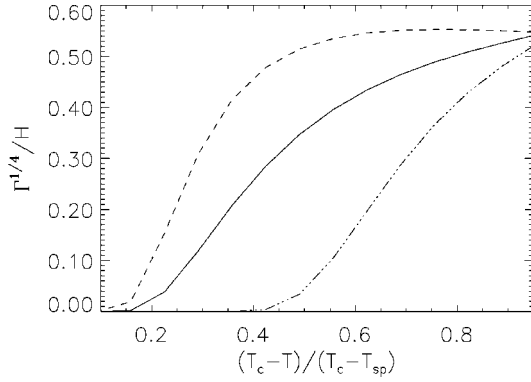
FIG. 9. $\Gamma^{1/4}$ divided by an assumed expansion rate of $H = 1 \ \text{fm}^{-1}$ as a function of temperature. The solid line shows the exact (numerical) result, the dashed line shows the thin-wall approximation, and the dotted line shows exact results for the modified potential.

FIG. 10. Correlation length of the chiral order parameter in the metastable state (l_f) and in the global minimum corresponding to an equilibrium transition (l_t). Solid lines correspond to the exact results, while dashed lines were obtained within the thin-wall approximation.

it is sufficient to raise F_b/T from the value of 2 (for the original V_{eff}) to 10. Following exponentiation, this leads to a reduction of Γ by a factor of almost 3000. The values of F_b/T for this modified potential, shown in Fig. 7, suggest stability of the metastable phase for all $x < 0.83$.

It is now a simple matter to obtain Γ, the nucleation probability per unit time and volume, and to determine the space-time scales for homogeneous nucleation. This decay rate must be compared with the expansion rate of the central region of a high-energy collision. Certain obvious conditions apply. For example, the critical radius R_c cannot exceed the horizon. Otherwise, the center of the bubble cannot be causally connected to its surface, and the hydrostatic balance of surface and volume energy is thus impossible. In addition, there is a time scale associated with a spontaneous coherent thermal fluctuation of energy E_c with a length-scale of R_c. If that time-scale is larger than the inverse expansion rate, bubble nucleation can be regarded as a slow process, and deep supercooling is to be expected. (This is the condition that $F_b/T \gg 1$ discussed above.) To our knowledge, these questions have not previously been addressed in studies of homogeneous nucleation in the QCD phase transition as found in hadronic collisions.

To simplify our considerations, we assume that the central rapidity region exhibits one-dimensional (longitudinal) Hubble flow [24] with an expansion rate (i.e. Hubble constant) $H = 1/t$, where t denotes proper time. Even in large nuclei, transverse expansion can increase the local expansion rate considerably when the system has cooled down to $T \approx T_c$ [25]. Reasonable expansion rates are $H \approx 0.1 - 1 \ \text{fm}^{-1}$ [9,25].

We have chosen $\Gamma^{1/4}/H$ as a measure for the comparison of nucleation and expansion [13]. The results shown in Fig. 9 assume an expansion of $H = 1 \ \text{fm}^{-1}$. When the nucleation rate is much larger than the expansion rate, it is reasonable to adopt standard thermodynamic techniques and to describe the phase transition by an idealized Maxwell construction [16]. Our results suggest that the Maxwell construction is not likely to provide a reliable description of the phase transitio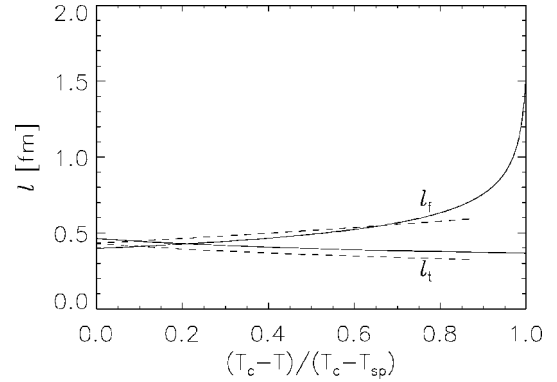n dynamics. While the results of Fig. 9 do not provide an unambiguous prediction for the fate of the metastable state, they do make it appear likely that the rapidly expanding system has an appreciable probability of remaining in the restored symmetry phase even close to the spinodal instability. Thus, at least some fraction of all heavy ion events should show traces of this non-equilibrium transition. This underscores the importance of the event-by-event analysis of data [6].

We now consider some potential consequences of a non-equilibrium transition associated with strong supercooling relative to an adiabatic transition. First, the character of the phase transition will certainly influence global observables and the expansion of the hot system. For example, a non-equilibrium transition is always associated with entropy production which can be as large as 30% [16]. This would be reflected in the multiplicity of hadrons in the final state. Moreover, phase coexistence in equilibrium leads to a distinct hydrodynamic expansion pattern which would be absent in a rapid non-equilibrium transition with strong supercooling. Since this issue has already received considerable attention in the literature [26], we refrain from a detailed discussion here.

Further, as discussed in [9], if the chiral condensate is "trapped" in the false minimum and supercooling persists close to the spinodal instability, the subsequent realignment in the chiral field in the direction of the true vacuum can generate strong coherent pseudoscalar fields, $\vec{\pi}$, which will eventually decay into a "beam" of coherent pions. The experimental situation will then be similar to that following an "instantaneous quench" of the restored symmetry phase [8].

Consider the behavior of the correlation length of the Φ-field. It is obvious from Fig. 1 that the curvatures of the effective potential at the minima Φ_f and Φ_t are rather different for $T < T_c$. Thus, the effective mass, $m_{\text{eff}}^2 = d^2 V_{\text{eff}}/d\Phi^2$, and the correlation length, $l = 1/m_{\text{eff}}$, of the field will also be different. In particular, if the rapidly expanding system supercools appreciably and if the order parameter is trapped in the metastable state, one can expect a clear increase of l.

In Fig. 10 we show l at Φ_f and at Φ_t as a function of the

degree of supercooling. The correlation length at Φ_f increases as the metastable minimum disappears. By contrast, there is a smooth decrease in the correlation length at the true minimum Φ_t (which would be the expectation value of Φ if the transition proceeded in equilibrium). In the present model l_f can exceed l_t by as much as a factor of 2–3, depending on the degree of supercooling. The precise values of l_f and l_t depend on the specific effective model adopted, but the qualitative observation that l_f increases dramatically as the system approaches the spinodal instability is general.

At the critical temperature, the thin-wall approximation leads to only one correlation length, $l_{tw} = \xi/2$, where ξ is the thickness of the critical bubble as given by Eq. (3.12). This is because the thin-wall approximation assumes both a small degree of supercooling and a small latent heat, i.e. a weak transition. Thus, the curvatures at Φ_f and at Φ_t coincide to leading order in ξ/R_c. To leading order in ξ/R_c and for $T_{sp} < T < T_c$, we find

$$W''(\phi_f) - W''(\phi_t) = -6|j|/a. \tag{4.1}$$

Correlation lengths in the thin-wall approximation are shown in Fig. 10 by the dashed lines. The splitting of l_f and l_t is described reasonably well (at least qualitatively) except close to the spinodal, where this approximation is most unreliable.

We note that the horizon, $1/H$, in expanding systems provides an upper bound on the correlation length; l_f cannot increase beyond the horizon. Thus, observable consequences can be expected only if the expansion rate diminishes near the spinodal. On the other hand, correlation lengths cannot become large if expansion rates are too small, e.g. $H < 0.1$ fm^{-1}, since the dynamics will no longer support strong supercooling.

As we have argued above, nucleation is not effective for small supercooling because F_b/T is large. The decay rate is then likely to be much smaller than the expansion time, and the system is likely to remain in the false vacuum. On the other hand, the approximations of homogeneous nucleation theory are likely to break down near the spinodal where the decay rate of the false vacuum becomes large. There, the condition $R_c \gg l_f$, inherent to nucleation theory, is no longer valid. If $R_c \approx l_f$, it makes little sense to think of a bubble as a coherent superposition of random thermal fluctuations of wavelength l_f in hydrostatic equilibrium with the surrounding symmetric phase. It may rather be more appropriate to treat fluctuations on the scale l_f as random thermal noise to be introduced into the classical equations of motion for the order parameter through, for example, a Langevin equation [27]. In short, our results suggest that homogeneous nucleation theory may never provide a suitable modeling of the chiral phase transition in particle collisions.

V. SUMMARY AND OUTLOOK

We have considered homogeneous bubble nucleation in a first-order chiral phase transition within an effective field theory approach to low-energy QCD, i.e. a linear σ-model coupled to quarks. Integrating out the quarks leads to an effective potential for the soft modes of the chiral fields (i.e.

the order parameter) with two competing minima for $T = T_c$, corresponding to a first-order phase transition. The approximation of this effective potential by a familiar Landau-Ginzburg form allowed us to obtain analytical results for critical bubble profiles and decay rates using the thin-wall approximation. Comparisons with exact numerical solutions, which do not employ the thin-wall approximation, suggest that the thin-wall approximation is not adequate for the description of high-energy hadronic collisions. Its use results in a significant underestimation of the size of critical bubbles. The effects of this error are then amplified in the calculation of the decay rate. Furthermore, the thin-wall approximation cannot be used to obtain the correlation length in the metastable state close to the spinodal.

Our results show a rapid decrease with temperature in the free energy of critical bubbles from infinity at the critical temperature to zero at the spinodal. Given the exponential dependence of Γ on F_b/T, this fact provides some justification for our crude treatment of the prefactor in Γ. Furthermore, it suggests that the metastable phase is likely to survive at temperatures such that $F_b \gg T$ is independent of the details of either the decay process or the expansion. Even the weak first-order transition considered here suggests the viability of the restored symmetry phase for $(T_c - T)/(T_c - T_{sp}) < 2/3$. As we have suggested, stronger transitions will allow the metastable state to survive even closer to the spinodal instability. The fate of the metastable state when $F_b < T$ is a more delicate issue and requires the comparison of the spatial/temporal scale, $\Gamma^{1/4}$, for critical thermal fluctuations to the typical expansion rate, H, expected in high-energy collisions. The small values of $\Gamma^{1/4}/H$ found in our calculations suggest that the phase transition is likely to proceed through spinodal decomposition rather than bubble nucleation for some fraction of all events (or some fraction of all rapidity bins). Our results certainly indicate that $\Gamma^{1/4}$ is not materially larger than H. This suggests the familiar idealized Maxwell construction of equilibrium thermodynamics is not appropriate for the description of phase transitions in high-energy heavy ion collisions. In fact, the relevance of nucleation theory for a possibly first-order chiral phase transition in high-energy collisions appears questionable. The conditions $F_b < T$ and $l_f < R_c$ leave at best only a small window of temperatures where nucleation might occur.

Although current knowledge is insufficient to identify the order of the QCD phase transition in hadronic collisions with certainty, it is still important to search for experimental indications of supercooling. In addition to more familiar indicators, we have shown that the correlation length in the supercooled metastable state can be substantially larger than that expected in an equilibrium transition if the degree of supercooling is large. Whether this can lead to observable consequences depends sensitively on the expansion rate of the system, H. Small H will not support deep supercooling, and the relevant correlation length will remain close to l_t, which is small. On the other hand, large H will set causality limits on the size of the correlation length at the false minimum, which cannot exceed the horizon $1/H$. It remains to be seen if there is a ''window'' of energy or projectile-target combination for which the predicted increase in the correlation length can be

observed. This speculation requires more detailed numerical studies of hydrodynamic expansion coupled to dynamical bubble nucleation (with realistic initial conditions) before definite predictions can be made.

The experimental observation of supercooling effects and spinodal decomposition would also be important as a matter of principle. Ideally, signatures of phase transitions should be order parameter related and should reveal properties of the equilibrium phase diagram. This is not the case for many of the signatures proposed for heavy ion collisions such as J/Ψ suppression and strangeness production. The interpretation of these signatures necessarily relies on theoretical estimates of reaction rates, and their connection to the thermodynamics of QCD is often far from clear. While the spinodal instability is not part of the equilibrium phase diagram, it is very close. Familiar experiments in condensed matter physics on a wealth of hysteresis phenomena (i.e., the analogue of superheating and supercooling) make it clear that spinodal instabilities can be studied on ''macroscopic'' time scales. The spinodal instability, if found, would probably represent the most direct information which relativistic heavy ion collisions can provide regarding the QCD phase transition.

Not surprisingly, our results indicate that the time scales for nucleation and expansion are not as well separated in high-energy hadronic–heavy-ion collisions as they are, for example, in the cosmological QCD phase transition. The assumption of a ''well-mixed'' phase, commonly employed in hydrodynamic calculations [26] and the opposite scenario of perfect capture of the order parameter in the metastable minimum [9] with subsequent spinodal decomposition, must be regarded as rough qualitative pictures. Furthermore, the possibility of significant supercooling indicated by our results suggests the necessity of including the effects of nonspherical bubble configurations as well. Bubble growth and bubble percolation in particular are likely to play an impor-

tant role in completing the transition. If the system evolves by strong supercooling followed by a rapid phase transition (due either to spinodal decomposition or nucleation of many small nonspherical bubbles which percolate), the constituent quarks will experience strong reheating due to the fact that they become essentially nonrelativistic. It would be interesting to seek experimental signatures for such ''reheating,'' which must be present if the quarks acquire mass instantaneously.

In our view, a realistic and quantitative discussion of those points requires numerical studies of the dynamical evolution of quarks (which constitute the heat bath) coupled to the chiral field. While initial investigations along these lines have been performed, e.g. Refs. [9,20], the effects of dynamical bubble nucleation have not yet been considered. Moreover, the use of oversimplified geometries did not allow for realistic velocity and temperature-density gradients, nonspherical bubble configurations, or bubble percolation. Work on these questions is in progress and will be reported elsewhere.

---

[1] E. V. Shuryak, Phys. Rep. **61**, 71 (1980); K. Kajantie and L. McLerran, Annu. Rev. Nucl. Part. Sci. **37**, 293 (1987); B. Müller, Rep. Prog. Phys. **58**, 611 (1995); J. Harris and B. Müller, Annu. Rev. Nucl. Part. Sci. **46**, 71 (1996); S. A. Bass, M. Gyulassy, H. Stöcker, and W. Greiner, J. Phys. G **25**, R1 (1999).

[2] J. C. Collins and M. J. Perry, Phys. Rev. Lett. **34**, 1353 (1975); E. Witten, Phys. Rev. D **30**, 272 (1984); J. H. Applegate and C. Hogan, *ibid.* **31**, 3037 (1985).

[3] J. Ignatius, K. Kajantie, H. Kurki-Suonio, and M. Laine, Phys. Rev. D **50**, 3738 (1994).

[4] L. Dolan and R. Jackiw, Phys. Rev. D **9**, 3320 (1974).

[5] PHOBOS Collaboration, B. B. Back *et al.*, Phys. Rev. Lett. **85**, 3100 (2000).

[6] R. Stock, in *NATO Advanced Study Workshop on Hot Hadronic Matter: Theory and Experiment, Divonne-les-Bains*, France, 1994; M. M. Aggarwal, V. S. Bhatia, A. C. Das, and Y. P. Viyogi, Phys. Lett. B **438**, 357 (1998); NA49 Collaboration, J. G. Reid, Nucl. Phys. **A661**, 407 (1999).

[7] I. N. Mishustin, Phys. Rev. Lett. **82**, 4779 (1999); H. Heisel-

berg and A. D. Jackson, nucl-th/9809013.

[8] A. A. Anselm and M. G. Ryskin, Phys. Lett. B **266**, 482 (1991); J. D. Bjorken, Int. J. Mod. Phys. A **7**, 4189 (1992); J. P. Blaizot and A. Krzywicki, Phys. Rev. D **46**, 246 (1992); K. Rajagopal and F. Wilczek, Nucl. Phys. **B399**, 395 (1993); **B404**, 577 (1993).

[9] O. Scavenius and A. Dumitru, Phys. Rev. Lett. **83**, 4697 (1999).

[10] M. A. Halasz, A. D. Jackson, R. E. Shrock, M. A. Stephanov, and J. J. Verbaarschot, Phys. Rev. D **58**, 096007 (1998); M. Stephanov, K. Rajagopal, and E. Shuryak, Phys. Rev. Lett. **81**, 4816 (1998); J. Berges and K. Rajagopal, Nucl. Phys. **B538**, 215 (1999); T. M. Schwarz, S. P. Klevansky, and G. Papp, Phys. Rev. C **60**, 055205 (1999); J. T. Lenaghan, Phys. Rev. D **63**, 037901 (2000).

[11] O. Scavenius, A. Mocsy, I. N. Mishustin, and D. H. Rischke, nucl-th/0007030.

[12] K. Enqvist, J. Ignatius, K. Kajantie, and K. Rummukainen, Phys. Rev. D **45**, 3415 (1992).

[13] M. Gleiser, E. W. Kolb, and R. Watkins, Nucl. Phys. **B364**, 411 (1991).

[14] J. S. Langer, Ann. Phys. (N.Y.) **41**, 108 (1967); **54**, 258 (1969); **65**, 53 (1971); J. S. Langer and L. A. Turski, Phys. Rev. A **8**, 3230 (1973); **22**, 2189 (1980).

[15] A. D. Linde, Nucl. Phys. **B216**, 421 (1983); **B223**, 544(E) (1983).

[16] L. P. Csernai and J. I. Kapusta, Phys. Rev. Lett. **69**, 737 (1992); Phys. Rev. D **46**, 1379 (1992); J. I. Kapusta, A. P. Vischer, and R. Venugopalan, Phys. Rev. C **51**, 901 (1995); P. Shukla, A. K. Mohanty, S. K. Gupta, and M. Gleiser, *ibid.* **62**, 054904 (2000).

[17] See, e.g., E. Laermann, Nucl. Phys. **A610**, 1C (1996).

[18] E. S. Fraga and C. A. A. de Carvalho, Phys. Rev. B **52**, 7448 (1995); D. G. Barci, E. S. Fraga, and C. A. A. de Carvalho, Phys. Rev. D **55**, 4947 (1997); S. Alamoudi, D. G. Barci, D. Boyanovsky, C. A. A. de Carvalho, E. S. Fraga, S. E. Jorás, and F. I. Takakura, *ibid.* **60**, 125003 (1999).

[19] M. Gell-Mann and M. Levy, Nuovo Cimento **16**, 705 (1960).

[20] L. P. Csernai and I. N. Mishustin, Phys. Rev. Lett. **74**, 5005 (1995); A. Abada and M. C. Birse, Phys. Rev. D **55**, 6887 (1997); I. N. Mishustin and O. Scavenius, Phys. Rev. Lett. **83**, 3134 (1999).

[21] R. D. Pisarski and F. Wilczek, Phys. Rev. D **29**, 338 (1984).

[22] J. Kapusta, *Finite Temperature Field Theory* (Cambridge University Press, Cambridge, England, 1989).

[23] S. Gavin, A. Gocksch, and R. D. Pisarski, Phys. Rev. Lett. **72**, 2143 (1994); Phys. Rev. D **49**, 3079 (1994).

[24] J. D. Bjorken, Phys. Rev. D **27**, 140 (1983).

[25] A. Dumitru, Phys. Lett. B **463**, 138 (1999).

[26] M. Kataja, P. V. Ruuskanen, L. D. McLerran, and H. von Gersdorff, Phys. Rev. D **34**, 2755 (1986); U. Ornik, F. W. Pottag, and R. M. Weiner, Phys. Rev. Lett. **63**, 2641 (1989); N. S. Amelin, E. F. Staubo, L. P. Csernai, V. D. Toneev, K. K. Gudima, and D. Strottman, *ibid.* **67**, 1523 (1991); A. Dumitru, U. Katscher, J. A. Maruhn, H. Stöcker, W. Greiner, and D. H. Rischke, Phys. Rev. C **51**, 2166 (1995); C. M. Hung and E. V. Shuryak, Phys. Rev. Lett. **75**, 4003 (1995); D. H. Rischke and M. Gyulassy, Nucl. Phys. **A608**, 479 (1996); J. Brachmann *et al.*, Phys. Rev. C **61**, 024909 (2000).

[27] M. Alford, H. Feldman, and M. Gleiser, Phys. Rev. D **47**, 2168 (1993); J. Borrill and M. Gleiser, *ibid.* **51**, 4111 (1995); C. Greiner and B. Müller, *ibid.* **55**, 1026 (1997); D. Boyanovsky, H. J. de Vega, R. Holman, S. Prem Kumar, and R. D. Pisarski, *ibid.* **58**, 125009 (1998).